Joint International Topical Meeting on Mathematics & Computation and Supercomputing in Nuclear Applications (M&C + SNA 2007)
Monterey, California, April 15-19, 2007, on CD-ROM, American Nuclear Society, LaGrange Park, IL (2007)

3D WHOLE CORE FINE MESH MULTIGROUP DIFFUSION CALCULATIONS BY DOMAIN DECOMPOSITION THROUGH ALTERNATE DISSECTIONS

José-Javier Herrero, Carol Ahnert and José-María Aragonés

Departamento de Ingeniería Nuclear; Universidad Politécnica de Madrid
C/ José Gutiérrez Abascal, 2; 28006 Madrid (Spain)
herrero@din.upm.es; carol@din.upm.es; arago@din.upm.es

ABSTRACT

The fine mesh diffusion formulation is extended to deal with multigroup 3-D problems in rectangular geometries. The formulation includes interface discontinuity factors per cell type, pre-calculated from transport solutions. The iterative scheme, aiming to an efficient parallel implementation in memory distributed multi-processors, is based on domain decomposition in the 4 possible sets of 4 neighbor quarters of assemblies. The alternate dissections achieve convergence to the exact boundary conditions, while attenuating high frequency noise. Whole core convergence is accelerated in the long wavelength effects by a consistent high-order analytical nodal solution performed by the ANDES solver. A neutronics - thermal-hydraulics iterative scheme is also developed to compute best estimate results, by coupling at the detailed cell-subchannel scale the COBAYA3 code with several TH subchannel codes. The numerical performance and convergence rates are verified by computing pin-cell scale solutions for the OECD/NEA/USNRC PWR MOX/UO_2 Core Transient Benchmark in 8 energy groups and heterogeneous assemblies. The cell-subchannel scale neutronics and thermal-hydraulics coupling, allows the verification of the effects of the detailed TH feedbacks on cross-sections and, thus, on fuel pin powers, calculated here for a 3D color-set of two different fuel types of the previous benchmark, using COBAYA3 and COBRA-3C.

Key Words: fine mesh diffusion, multigroup, multiscale, multiphysics, domain decomposition.

1. INTRODUCTION

The fine mesh diffusion formulation was already developed and implemented in 2D and two-groups with extended use applied to the operating Spanish PWR NPPs. It included interface discontinuity factors by cell type to correct for the transport and heterogeneity effects and it was accelerated by a nodal solution [1]. Neutronics and thermal-hydraulics coupling was performed at nodal/channel scale, with the possibility of off-line and non-iterative pin-cell/sub-channel scale studies of isolated fuel assemblies [2]. Those methods were capable of 2D core calculations in two energy groups at the fine mesh scale, and in 3D and two groups, or in one and a half groups, at the nodal scale.

In this work we have pushed forward the improvement of the fine mesh method, at the pin-cell scale, to include the third dimension and a higher number of energy groups, as well as the

capability of iterative coupling with thermal-hydraulical calculations at the subchannel level, including the feedbacks on the cross sections.

We present the very last results of this new implementation applying the method to the current 3D PWR MOX/UO_2 Core Transient Benchmark designed to assess full core simulators using fixed thermal-hydraulical conditions; and we show some first results on coupled simulations at the pin-cell level for an isolated color-set from that benchmark.

2. THE FINE-MESH FINITE DIFFERENCES DIFFUSION METHOD

2.1. General equation discretization

Beginning from the k eigenvalue stationary diffusion equation which can be expressed as:

$$\nabla\cdot(-D^g\cdot\nabla\phi^g)+\Sigma_{abs_p}{}^g\cdot\phi^g+\sum_{g'\neq g}\Sigma_{scat_p}{}^{g\to g'}\cdot\phi^g=\sum_{g'\neq g}\Sigma_{scat_p}{}^{g'\to g}\cdot\phi^{g'}+\frac{1}{k_{eff}}\cdot\sum_{\forall g'}\nu\Sigma_{fiss_p}{}^{g'\to g}\cdot\phi^{g'} \quad (1)$$

The eigenvalue diffusion multigroup equations are discretized in fine-mesh cells by a centered finite difference involving cell discontinuity factors, diffusion coefficients and mesh-size values for the cells inside the local subdomain, as well as the current-to-flux ratios in the boundaries. Moving most of the fission source to the left side, by applying a Wielandt shift represented by ω [8], and using the following definitions:

$$\left.\begin{aligned}\frac{\Delta^g_{n-p}\cdot idf^{\,g}_{p\to n}}{h_n}=\alpha^{\,g}_{p\to n}\quad;\quad \Sigma_{scat}{}_p^{\,g'\to g}+\frac{\omega}{k_{eff}}\nu\Sigma_{fiss}{}_p^{\,g'\to g}=\beta_p^{g'\to g}\\ \sum_{n=1}^{6}\frac{\Delta^g_{n-p}\cdot idf^{\,g}_{n\to p}}{h_n}+\Sigma_{abs}{}_p^{\,g}+\sum_{g'\neq g}\Sigma_{scat}{}_p^{\,g\to g'}-\frac{\omega}{k_{eff}}\nu\Sigma_{fiss}{}_p^{\,g\to g}=\beta_p^{g}\end{aligned}\right\} \quad (2)$$

Here, delta terms represent the streaming discretization that couples the equation between the node *p* and its, generally, six neighbours represented by index *n*. The term *idf* stands for the interface discontinuity factors which account for transport and mesh discretization approximations [1]. The streaming terms are developed giving:

$$J^{\,g}_{p,n}=\frac{2\cdot D^g_p\cdot D^g_n}{D^g_p\cdot h_n\cdot idf^{\,g}_{p\to n}+D^g_n\cdot h_p\cdot idf^{\,g}_{n\to p}}\cdot(\pm idf^{\,g}_{n\to p}\cdot\phi^g_p\mp idf^{\,g}_{p\to n}\cdot\phi^g_n)=\Delta^g_{n-p}\cdot(\pm idf^{\,g}_{n\to p}\cdot\phi^g_p\mp idf^{\,g}_{p\to n}\cdot\phi^g_n) \quad (3)$$

Where the first set of signs is for currents coming from a neighbour n > p, and vice versa. On the other side, the interface currents for the boundary conditions are expressed:

$$J_{p,n}^{g} = \frac{\phi_p^g}{\dfrac{idf_{p\to n}^{g}}{J_{p,n}^{g}/\phi_{p,n}^{g}} \pm \dfrac{h_p}{2\cdot D_p^g}} \tag{4}$$

Note that the expression for the current in a boundary depends only in the current to flux ratio $J_{p,n}^{g}/\phi_{p,n}^{g}$ on the interface, and geometrical and material properties of the cell besides that boundary, so each subdomain can be solved independently from each other and the coupling terms between them enter the linear system in the main diagonal. The general linear system of equations takes the form:

$$\begin{bmatrix} \ddots & & \ddots & & \ddots & \\ \cdots & -\alpha_{p\to n}^{g} \cdots & -\beta_p^{1\to g} \cdots & \beta_p^{g} \cdots & -\beta_p^{G\to g} \cdots & -\alpha_{p\to n'}^{g} \cdots \\ & \ddots & & \ddots & & \ddots \end{bmatrix} \begin{pmatrix} \vdots \\ \phi_p^g \\ \vdots \end{pmatrix} = \frac{1-\omega}{k_{eff}} \begin{pmatrix} \vdots \\ \nu\Sigma_{fiss\,p}^{g\to g} \cdot \Phi_p^g \\ \vdots \end{pmatrix}$$

Resulting in a general heptadiagonal matrix where the main diagonal is composed by full block-matrices which dimension is the number of energy groups, coupling inside each cell scattering and fission events. The matrix has the structure of a Z-matrix, with non-positive non-diagonal terms, non-symmetric as it includes interface discontinuity factors, and whose diagonal dominance cannot be assured because of the boundary conditions of any sign in the diagonal Δ_{n-p}^{g} terms and the imbalance in scattering and fission reactions for the different energy groups inside a cell. This structure is still adequate for certain preconditioning schemes and Krylov methods, namely BICGSTAB or GMRES [7], where the full energy spectrum is computed simultaneously in the domain avoiding, for instance, scattering rebalancing issues.

The previous system can be solved directly with the present subspace projection based iterative solvers, and it is feasible to use domain decomposition and take advantage of parallelization techniques. The chosen approach is to form the subdomains previously to the matrix system formulation, and casting the mathematical relation between each of them by means of the boundary conditions of each subdomain, which can be current to flux ratios on interfaces or directly the interface absolute currents when there is not a fission source.

In previous works [6] it was realized that the current to flux ratios – J/ϕ ratios from now on – are the best boundary conditions to apply for the equation solving, as they are independent of the normalization and dimensionless. For subdomains containing a fission source this will be the condition to apply as the normalization comes from that source; whereas for subdomains representing reflector regions, the normalization has to come from the boundary conditions itselfs, so absolute currents have to be used if seeking the correct flux level corresponding to the full core problem.

When J/ϕ ratios are used they can appear decreasing the main diagonal value, thus producing diagonal dominance loss; on the other hand, when currents are used they are passed to the right hand side of the linear system making it heterogeneous and giving the possibility of solving it

with the same iterative solvers. Diagonal dominance is a very desirable property of M-matrices and permits to assure the existence of certain incomplete factorizations for preconditioning [7]. This dominance will depend on the subdomain formed, for instance, if it consisted in an assembly where a control rod is inserted, J/ϕ ratios would be large and inward, and as a result the diagonal value could be decreased if it is accomplished that:

$$\left| \frac{idf^{g}_{p\to n}}{J^{g}_{p,n}/\phi^{g}_{p,n}} \right| > \left| \frac{h_p}{2 \cdot D^{g}_{p}} \right| \tag{5}$$

The contrary can be observed for an assembly next to a control rod and the reflector, where the diagonal dominance is always improved by these terms with outward currents.

The other source of diagonal dominance loss is the introduction of an spectral shift to accelerate the inverse power iteration, this value always decreases the diagonal value, and also have a negative effect on the iterative solver convergence, thus an equilibrium has to be found between the amount of shift applied and the convergence deceleration, which can end up in a solver failure for BiCGSTAB.

As a result, only GMRES iterative solver for general matrices can assure enough stability in most situations. To use this solver is advisable to apply a preconditioner, given the matrix structure of block diagonals it is guessed that a block diagonal Jacobi or ILU factorization could be preconditioners good enough preconditioner to get acceptable convergence speeds.

In practice, only GMRES with ILU preconditioning and BiCGSTAB with simple Jacobi preconditioning have been tested, and in this case BiCGSTAB results to be quite faster than the preconditioned GMRES. In conclusion, BiCGSTAB is preferred whenever possible, and GMRES remains as a second option that assures convergence in those subdomains where the linear system has a worse behavior.

The power iteration used to solve the eigenvalue problem is accelerated by performing a one group solution after each source iteration in multigroups, and both solution are further accelerated by introducing a spectral shift. Moreover, the one group acceleration does not represent a threat to the system stability, so it is always safer to accelerate the solution with this method than with the spectral shift, and the computing time becomes comparable as the one group collapsing balances the BiCGSTAB deceleration by the shift. All of them have been used depending on the subdomain characteristics.

Going over the issue of convergence dependence on the cell size, the results show that taking 8 cells radially per fuel pin yields a very good numerical solution to the diffusion equation. Nevertheless, in this method, only one cell per fuel pin will be considered as meshing effects are supposed to be contained in the interface discontinuity factors obtained from transport solutions, which also correct the heterogeneity and anisotropy effects not considered in diffusion theory.

In the axial direction even 5 cm length cells are enough to get good results. Thought, care must be taken if the problem considers control rods partially inserted or thermal-hydraulical grids to improve mixing; again, interface discontinuity factors could be used if necessary.

2.2. Domain decomposition scheme through alternate core dissections

The solution scheme (Figure 1) for the whole core 3D fine-mesh problem is based on domain decomposition in the radial directions, aiming also to an efficient parallel implementation in memory distributed multi-processors.
The full axial direction is kept in the same domain in order to couple properly with thermal-hydraulics and alternate dissections in the 4 possible sets of 4 neighbor quarters of assemblies are required to accelerate the convergence to the exact boundary conditions of the subdomains, while attenuating the high frequency noise. In this scheme, the boundary conditions for the next dissection are computed on the centerplanes of the subdomain, thus reducing significantly the numerical errors on the iteratively updated boundary conditions.

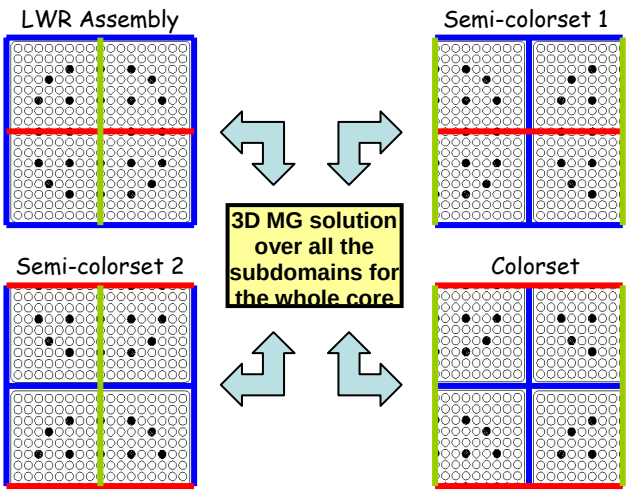

Figure 1. Domain decomposition by alternate dissections

In first instance, it can be considered that the J/ϕ ratios in the middle of each assembly will be low and forming a simple pattern because of the inherent symmetry; however this ratios will be of importance in the planes between different assemblies as there can be no quarter symmetry at all so the resulting pattern can be complex. Therefore, fewer iterations will be needed to converge to a good estimation of the boundary conditions in the assembly centerplanes, while a higher number of iterations will be needed to get good values in the centerplanes of colorsets.

The other two types of configurations called semi-colorsets are also of importance, because subdomain problems would not reach full convergence without including them. The reason is that if only assemblies and colorsets configurations are considered, then for the next iteration the borders of the same centerplanes are always mixed from two subdomains solved separately, so if a perturbation is formed along these lines it will remain and even oscillate on these extremes.

The core dissections in semicolorsets make possible to converge these borders as their solutions are taken just in the center of the domain, thus yielding the best possible fine-mesh solution and lowering those high frequency perturbations along the lines. As a conclusion, the four kinds of dissections in subdomains are needed to get a fully converged solution since they complement each other.

In order to compute the J/ϕ ratios in the centerplanes for the next iterations two levels of approximation are taken. When the centerplane is in between to cells, the general second order central difference can be taken, including the interface discontinuity factors if present. Otherwise, the centerplane can be encountered in the middle of a cell, where the J/ϕ ratio cannot be computed with the same degree of accuracy, the chosen solution consists in a simple averaging of the currents on the interfaces of the cell, so the approximation is linear of first order.

This way of obtaining the boundary conditions have shown to reach convergence in the overall method, although it could be possible to compute all the boundary conditions with second order accuracy if needed, that would make necessary to duplicate the boundary conditions for centerplanes in the middle of cells for assemblies of an odd number of pins. The convergence behaviour is shown in Figure 2 across a face between elements for a problem of three by three reflected assemblies, it is seen how the absolute difference from the reference value is gradually decreased when the subdomains formed take this face inside their center.

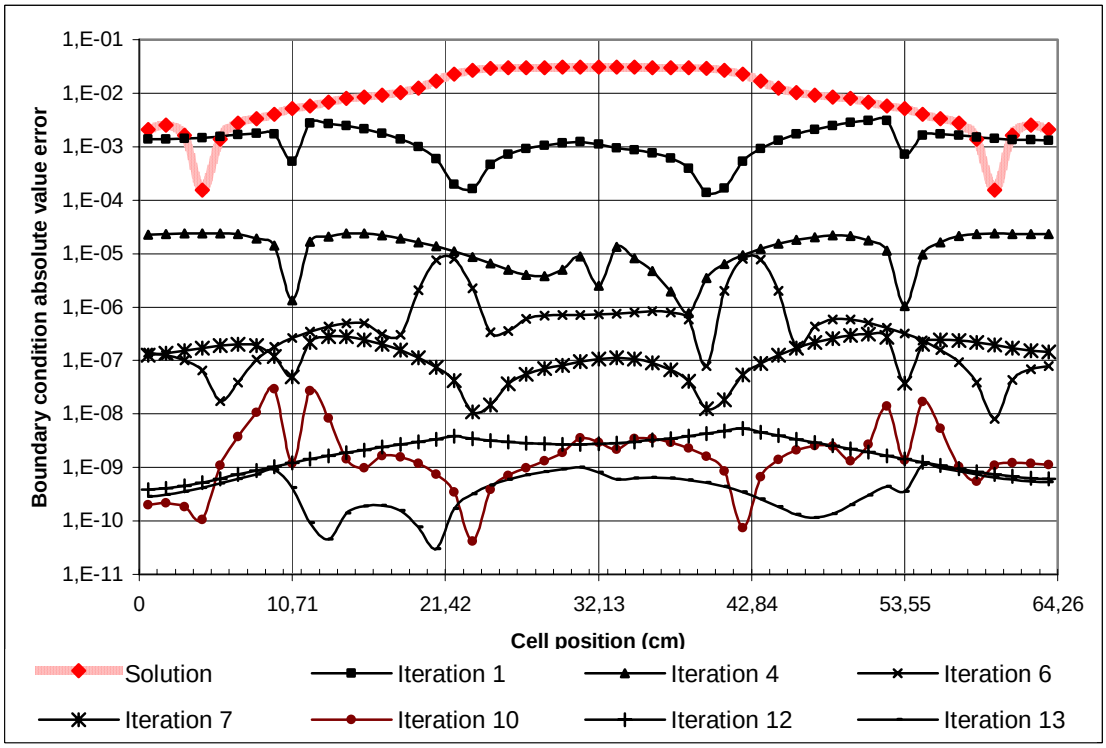

Figure 2. Convergence behavior of the boundary conditions for reflected assemblies

It is remarkable the appearance of discontinuities in the error, corresponding with the previously mentioned extremes of the computed faces where the numerical perturbations can appear if not performing the four decompositions. These extremes are marked with the vertical lines which coincide with the divisions of the assemblies in two nodes.

2.3. Whole core nodal acceleration

Whole core convergence is accelerated in the long wavelength effects by a consistent high-order analytical nodal solution performed by the ANDES solver [3], after each sweep over all the 3D subdomains. For a FMFD solver based in domain decomposition, a nodal acceleration is needed because of two reasons.

Firstly, in the case of trying to compute the solution for a commercial PWR at a pin level, numerical perturbations would take a huge number of iterations to travel from some part of the reactor to the opposite one, so the behaviour of the fine mesh is not desirable for the long range effects in the computed solution. Thus, it is useful to perform a solution in a coarser scale that can transport long wavelength effects from one discrete node to other in a few number of faster iterations.

Next, the solution of this coarse mesh iteration would be reflected in the next fine mesh iteration by modifying the boundary conditions with the nodal solution and updating the reference fission sources. In practice, the difference between the J/ϕ ratio computed from the fine mesh solution and the one obtained from de nodal solver is calculated for each node lateral face, afterwards this difference is added over each cell face corresponding to that nodal faces without interpolation and applying a damping to lower the values change.

When convergence is reached both solutions take the same values and the correction disappears, actually the difference is neglected if its value is less than a fraction of the J/ϕ ratio to avoid numerical oscillations. The absence of polynomial interpolation has turned out to be enough to accelerate the fine mesh solution in simple cases and it avoids changing the boundary conditions detailed profile with the nodal solution which cannot represent that shape correctly.

Secondly, if we take into account that the neutronics solution has to be normalized to a determined flux level or power level in the domain of interest; it is clear that the power level in each subdomain is unknown in the beginning; as a result we do not know the power distribution in the core. With independence of this point, the neutronic solution could be achieved without normalization, as the boundary conditions are independent of the flux level, as they are ratios between two magnitudes.

This is not the case when reflector is present in the problem, for the case of domains formed by reflector material, there is not presence of a fission source and the linear system built for the computation becomes homogeneous leading to an infinite number of solutions over the kernel of the system.

In practice, is preferable to be able to compute a unique value with the same methods that are being used with the subdomains containing fuel; so as to get an heterogeneous linear system, the boundary condition in faces of the reflector subdomain corresponding to physical neighbours – this means not being the boundary conditions of the overall problem as for instance J/ϕ ratios for void, reflective or infinite reflector boundary conditions – are taken like the boundary

currents, and instead of being introduced in the main diagonal of the system matrix they are taken to the right hand side of the system filling the independent term with not null values.

Following the previous explanation, it turns out that these new values are not independent of the flux or power renormalization in the subdomains, so this must be consistent in the full problem. Besides, it is necessary to take the system solution to the correct power level, moreover, when a thermal-hydraulical coupling will be also considered in the near term.

Next figure 3 compares the convergence of the fission source for the same problem solved directly without domain decomposition, applying the domain decomposition but not accelerating with a nodal solution, and improving the scheme with nodal acceleration. This case is the best achievable as it is almost symmetric and no complex patterns of local boundary conditions are encountered.

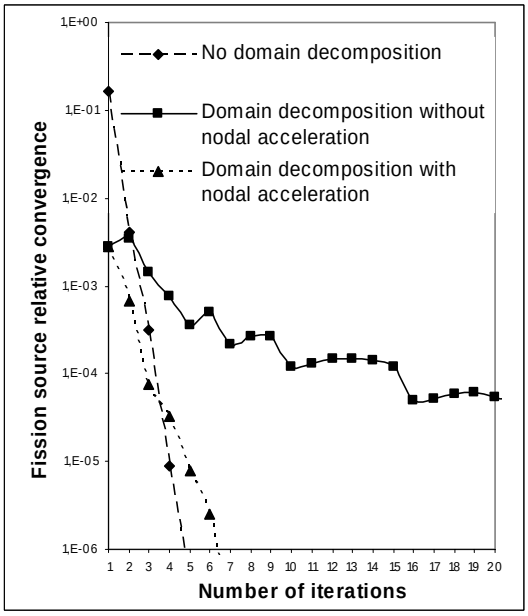

Figure 3. Convergence of fission source with domain decomposition

When the material composition includes situations such as only one extracted control rod in the core, the J/ϕ ratios have an internal structure inside each nodal face, current heterogeneity factors applied to the nodal solver only consider flat profiles in the face for the transversal leakages currents. At this time more complex patterns of currents are being used to get heterogeneity factors which do not have to contain a correction because of the local interface currents profile, thus improving the acceleration in difficult problems. Until a better computation of the heterogeneity factors is available, a damping on the boundary conditions interpolation is applied to avoid oscillations that do not permit full convergence for these complex cases.

2.4. Coupling and feedback with thermal-hydraulics at the pin-cell subchannel scale

The thermal-hydraulics couplings and feedbacks are done at the fuel rods and subchannels scale for each 3D subdomain of whole core height. The pin power solution is passed to the TH code, which combines it with the geometrical and material descriptions of rods and subchannels and, in the future, with the iteratively updated boundary conditions on each subdomain, namely the cross flows between subchannels, to calculate the fuel, clad, and coolant thermodynamical state and to pass it back to the neutronics until iteration convergence within each subdomain. Several available TH subchannel codes, such as COBRA-3C, COBRA-TF and FLICA4 are being interfaced for this coupling [4].

Figure 4 shows convergence rates for a colorset from the benchmark used to test the code, reflective boundary conditions were used with 152 axial cells of around 2,5 cm in the axial direction and 1,26 cm in the radial direction and 8 energy groups. A damping in the variables has not been used and all the problems converge to less than 1 W/cm^3 per cell, though the rates are different, depending on the use of a detailed thermal-hydraulical solution, or an averaged one.

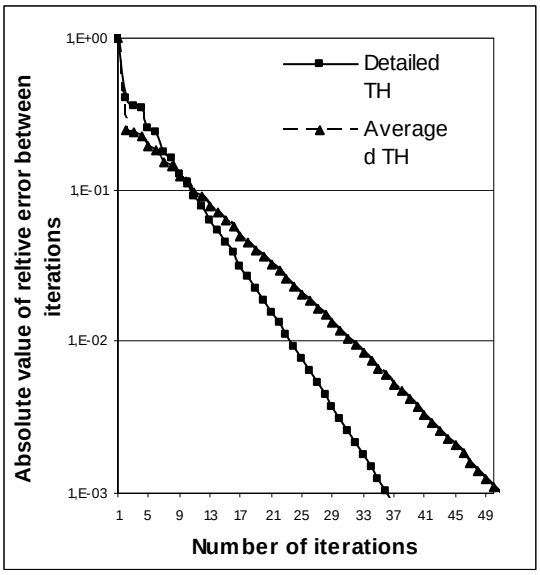

Figure 4. Convergence of neutronics and thermal-hydraulics coupling

Regarding a steady state calculation, the effect of feedback over the inverse power iteration is in a way similar to the effect of boundary conditions updating in the domain decomposition. If we express the inverse power iteration to perform like:

$$\vec{v}_i = A(\vec{v}_{i-1})^{-1} \cdot \lambda_{i-1} \cdot \vec{v}_{i-1} \qquad (6)$$

Where *i* is the iteration index, and it has been made explicit the feedback effect of the cross sections over the linear system matrix *A*. The iterative procedure assures that the values of λ and $\vec{v}$ converge to the biggest eigenvalue and a vector contained in the subspace associated to that value, which is the fission source distribution [8]. But each feedback iteration produces a change in the spectrum of the matrix and in the associated subspaces so each feedback iteration changes the direction in which $\vec{v}$ would converge, e.g. the fission source distribution.

This is a problem, as there is no way to assure that the linear system matrix will converge to the one that minimizes these spectral changes when the iteration is non-linear and a damping is applied over the thermalhydraulical conditions to accelerate convergence. Although in practice that is the case, and it permits to get the true power and thermal-hydraulical distributions in the assembly or colorset.

For the case of isolated assemblies and colorsets with reflective boundary condition with TH feedback, a proper approach to the convergence criteria had to be programmed so as to get to the solution in a few number of iterations. It was observed that there was an exponential convergence of the cell power error, and a fission source iteration tolerance had to be adapted in each step of the iteration, as very slow convergence would be obtained if computing a fully converged fission source on each step.

This coupling opens the door to the application of threading in the feedback iteration over each subdomain. The idea is to solve the problem in a dual core processor, as the neutronics are being calculated with the last thermal-hydraulical solution available in one of the cores, the thermal-hydraulical conditions are being recalculated with the last neutronics solution available, so we

are converging over linear systems whose associated subspaces are closer and closer to the one where the spectral distribution does not change at the end.

3. IMPLEMENTATION OF THE COBAYA-3 CODE

The method discussed above has been implemented in a new code, named COBAYA3, which includes solvers of the LAPACK and SPARSKIT libraries for the linear discretized systems and least-squares fitting problems. Code development is oriented to achieve the maximum degree of parallelization in the simultaneous solution of the different subdomains in different processors, with data inter-communication limited to a few neighbour nodes in a distributed memory architecture. The OpenMPI library is being used for this purpose.

Since each subdomain can be solved independently, and the information stream can be carried out in a decentralized manner to a neighbor processor for the next iteration, these characteristics make it suitable for the use of networked computers where each one solves a different subdomain simultaneously improving performance.

There are two ways of implementing the code parallelization, in case of the number of computers available are a few, a master process must be present which receives and sends the different solutions and boundary conditions to the different processors and computes the nodal acceleration solution. If a big number of processors are available, around 300, it is possible to perform a full iteration over all the core simultaneously and there is no need to send or receive boundary conditions and initial guess fluxes from the master process, which now only computes the nodal solution.

In this later case, the best advantages of the parallelization scheme are obtained, as the boundary conditions and initial guesses are passed using MPI to the neighbour processors, thus minimizing the information transitions and getting a faster solver. Even initial guesses can be omitted and only the boundary conditions could be passed so the information transport to information computed ratio becomes really low as a parallelized code demands.

The COBAYA3 code is memory consuming: for instance, a typical subdomain − formed by a single PWR assembly of 17x17 pin-cells divided in 320 axial cubic elements with 8 energy groups − requires 5.6 MB for the fine-mesh flux unknowns in double precision. The linear system reduces to a sparse matrix with all the diagonal blocks of 8x8 energy groups and six secondary diagonals, resulting in 79 MB of memory. And this amount is about doubled by the cross sections feedback parameters, burnup, detailed concentrations of main isotopes, geometrical values and auxiliary variables of the neutronics and TH problems. Finally, we have to multiply this by the number of fuel and reflector assemblies in the whole core, which is around 220 in a PWR; so that the total memory required is about 35 GB, largely exceeding the maximum available in desktop PC's and workstations. This is one further reason, in addition to the computing time, for the parallelization of the solver in a distributed, yet efficient, way among several high-speed networked desktops or in massively parallel supercomputers with about 300 dedicated nodes of 2 processors and 1 GB memory.

Although computational time could be of the same order independently of whether we performed domain decomposition or we used a parallelized full solver for the system, this way of computing the neutronics permits the explicit coupling with different subchannel TH codes. Ideally, we would use the same number of computers as the maximum number of subdomains that we could encounter forming a grid and sharing the information with their topological neighbours.

4. NUMERICAL VERIFICATION

The COBAYA3 code performance has been tested by computing pin-cell scale solutions for several 2D and 3D model problems, including assemblies, color-sets, multi-assemblies and mini-cores with pin-cell cross sections in 2 and 8 energy groups obtained from several NSC-NEA/OECD Benchmarks. The first results obtained for the 2D steady states at HZP of the whole core problems in the PWR MOX/UO_2 Rod Ejection Transient Benchmark in 8 energy groups are in quite good agreement with the reference published solutions [5]. These cases were chosen to perform the numerical verification of the code as an assembly heterogeneous cross sections library was presented in multigroups. It must be taken into account that heterogeneity factors were not delivered with this library so the results are only qualitatively comparable with those of the benchmark and only with the diffusion calculations.

To probe the method convergence for a full scale problem, the solution for the two-dimensional problems with fixed thermal-hydraulical conditions have been computed and compared with the provisional results obtained with PARCS and DeCART. Here we show for comparison the k effective eigenvalue for the ARO state with different meshings.

Table I. Comparison for HZP ARO 2D state PWR MOX/UO_2 Core Transient Benchmark

	PARCS 2G	DeCART MG	COBAYA3 8G (1 cell / pin)	COBAYA3 8G (2 cells / pin)
K_{eff} (difference PARCS)	1.06379	1.05852	1.06256 (123 pcm)	1.06335 (43.2 pcm)

In the following figures radial peaking factors F_q are shown for a colorset formed by a UOX assembly 4.2% enrichment and 35 GWd/tHM and a MOX assembly 4.3% 0.15 GWd/tHM from that benchmark, this last one on the first and last quadrants; peaking factors are taken at the axial level where the F_z reaches its maximum for each case. Materials are chosen to get a notable tilt in the power and the thermal-hydraulical conditions are that of the nominal state with 18.43 MW per assembly.

0.0	1.792	1.655	0.0	1.611	1.629	0.0	1.392	1.640
1.792	1.692	1.637	1.613	1.612	1.628	1.687	1.865	1.629
1.655	1.637	1.619	1.607	1.610	1.628	1.687	1.866	1.630
0.0	1.613	1.607	0.0	1.607	1.628	0.0	1.393	1.641
1.611	1.612	1.610	1.607	1.613	1.631	1.695	1.874	1.632
1.629	1.628	1.628	1.628	1.631	0.0	1.721	1.898	1.638
0.0	1.687	1.687	0.0	1.695	1.721	1.825	1.475	1.674
1.392	1.865	1.866	1.393	1.874	1.898	1.475	1.582	1.544
1.640	1.629	1.630	1.641	1.632	1.638	1.674	1.544	1.606
1.117	1.111	1.112	1.118	1.109	1.102	1.097	1.092	1.075
1.270	1.235	1.236	1.272	1.233	1.212	1.183	1.149	1.092
0.0	1.337	1.340	0.0	1.349	1.324	1.248	1.183	1.097
1.364	1.323	1.328	1.385	1.387	0.0	1.324	1.212	1.102
1.375	1.334	1.338	1.390	1.363	1.387	1.349	1.233	1.109
0.0	1.379	1.382	0.0	1.390	1.385	0.0	1.272	1.118
1.378	1.336	1.338	1.382	1.338	1.328	1.340	1.236	1.112
1.377	1.335	1.336	1.379	1.334	1.323	1.337	1.235	1.111
0.0	1.377	1.378	0.0	1.375	1.364	0.0	1.270	1.117

0.0	1.779	1.639	0.0	1.592	1.606	0.0	1.359	1.587
1.779	1.678	1.622	1.595	1.593	1.606	1.657	1.819	1.577
1.639	1.622	1.602	1.589	1.591	1.605	1.657	1.819	1.577
0.0	1.595	1.589	0.0	1.586	1.604	0.0	1.360	1.587
1.592	1.593	1.591	1.586	1.591	1.606	1.663	1.826	1.578
1.606	1.606	1.605	1.604	1.606	0.0	1.687	1.848	1.583
0.0	1.657	1.657	0.0	1.663	1.687	1.783	1.435	1.615
1.359	1.819	1.819	1.360	1.826	1.848	1.435	1.531	1.485
1.587	1.577	1.577	1.587	1.578	1.583	1.615	1.485	1.540
1.080	1.074	1.075	1.081	1.072	1.064	1.057	1.050	1.031
1.235	1.201	1.202	1.237	1.198	1.176	1.146	1.109	1.050
0.0	1.307	1.310	0.0	1.317	1.291	1.214	1.146	1.057
1.336	1.296	1.301	1.356	1.358	0.0	1.291	1.176	1.064
1.349	1.308	1.312	1.364	1.336	1.358	1.317	1.198	1.072
0.0	1.354	1.357	0.0	1.364	1.356	0.0	1.237	1.081
1.353	1.311	1.313	1.357	1.312	1.301	1.310	1.202	1.075
1.353	1.310	1.311	1.354	1.308	1.296	1.307	1.201	1.074
0.0	1.353	1.353	0.0	1.349	1.336	0.0	1.235	1.080

Figures 5A and 5B. Power peaking factors F_q with detailed thermal-hydraulics (A, left) and averaged thermal-hydraulics (B, right)

A comparison has been established between the solution with detailed subchannels for the COBRA-3C code and averaging the powers and thermal-hydraulical conditions per node for this solver, while maintaining the neutronics heterogeneity. This figures probe the importance of a detailed TH solution accompanying the detailed neutronics calculation. Table II exposes the differences in the most important values of both solutions.

Table II. Main differences between averaged an detailed thermal-hydraulics

	Detailed solution	Averaged solution (difference)
F_q	1.898	1.848 (0.050)
$F_{\Delta H}$	1.423	1.414 (0.009)
F_z	1.459	1.426 (0.033)
K_{eff}	1.04773	1.04979 (206 pcm)

5. CONCLUSIONS

The generalized fine-mesh diffusion formulation has been extended to multigroup 3-D problems in rectangular geometries; a complete domain decomposition scheme in 4 alternate dissections has been implemented, which has the potential for efficient parallel implementation in memory distributed multi-processors.

The implementation in the new COBAYA3 code and its first proof-of-principle applications has shown how the alternate dissections achieve quite effectively convergence to the exact boundary conditions, and how a consistent analytical nodal solution, performed by the ANDES solver, accelerates convergence to the whole core solution.

The developed of a neutronics and thermal-hydraulics coupling scheme, at the detailed cell-subchannel scale, allows the integration of COBAYA3 with several TH subchannel codes to asses the effects of the detailed TH feedbacks.

Ongoing work is to complete and test the effective parallelization of the COBAYA3 code in distributed networks of desktops and in massively parallel supercomputers, for the practical solution of whole 3D LWR core problems in multigroups and with coupled detailed thermal-hydraulics; the generalization of the solver to include kinetics; the improvement of the heterogeneity factors calculation for the nodal solver; and the generation of interface discontinuity factors from transport solutions to test more asymmetries in the linear systems formulation.

ACKNOWLEDGMENTS

This work is part of the ongoing PhD thesis of the first author and is partially funded by the EC Commission under the 6th EURATOM Framework Programme, within the RTD Integrated Project NURESIM "European Platform for Nuclear Reactor Simulations", contract No. 516560 (FI6O). It is also funded by the Spanish Education and Science Ministry under the FPU Programme for teaching and researching formation under grant AP2005-0667.

REFERENCES

1. J.M. Aragonés, C. Ahnert, "Linear-Discontinuous Finite-Difference Formulation for Synthetic Coarse-Mesh Few-Group Diffusion Calculations", *Nucl. Sci. & Eng.,* **94**, pp. 309-322 (1986).
2. J.M. Aragonés, C. Ahnert, O. Cabellos, N. García-Herranz, V. Aragonés-Ahnert, "Methods and Results for the MSLB NEA Benchmark using SIMTRAN and RELAP-5", *Nuclear Technology* **146**, pp. 29-40 (2004).
3. J.A. Lozano, J.M. Aragonés, N. García-Herranz, "Development and Performance of the Analytic Nodal Diffusion Solver ANDES in Multigroups for 3D Rectangular Geometry", submitted to *M&C/SNA-2007,* Monterey (this Conference) (2007).
4. P. Coddington, N. Crouzet, D. Cuervo, J. Jimenez, E. Royer, O. Zerkak, "LWR Multi-Physics Developments and Applications within the NURESIM European Project", submitted to *M&C/SNA-2007,* Monterey (this Conference) (2007).
5. T. Kozlowski, T. Downar, "OECD/NEA and US-NRC PWR MOX/UO2 Core Transient Benchmark", Purdue University, https://engineering.purdue.edu/PARCS/MOX_Benchmark (2003-2006).
6. Carolina Ahnert Iglesias, *Desarrollo y Validación de Métodos de Cálculo de Núcleos Heterogéneos de Reactores de Agua Ligera*, PhD thesis, Madrid (Spain) (1985).
7. Y. Saad. *Iterative Methods for Sparse Linear Systems*, *2nd edition*. SIAM, Philadelpha, PA (2003).
8. Y. Saad. *Numerical Methods for Large Eigenvalue Problems*. Halstead Press, New York (1992).